J. Appl. Comput. Mech., 8(3) (2022) 949-961
DOI: 10.22055/JACM.2021.34993.2533

ISSN: 2383-4536
jacm.scu.ac.ir

Shahid Chamran University of Ahvaz

Journal of Applied and Computational Mechanics

Research Paper

MHD Non-Newtonian Fluid Flow past a Stretching Sheet under the Influence of Non-linear Radiation and Viscous Dissipation

Ram Prakash Sharma[1], Sachin Shaw[2]

[1] Department of Mechanical Engineering, National Institute of Technology Arunachal Pradesh, Yupia, Pampum Pare District, Arunachal Pradesh – 791112, India, Email: rpsharma@nitap.ac.in

[2] Department of Mathematical and Statistical Sciences, Botswana International University of Science and Technology, Private Bag 16, Palapye, Botswana, Email: sachinshaw@gmail.com

Received September 11 2020; Revised December 03 2020; Accepted for publication January 28 2021.
Corresponding author: R.P. Sharma (rpsharma@nitap.ac.in)

Abstract. This work reports the heat and mass transfer of the 2- D MHD flow of the Casson and Williamson motions under the impression of non-linear radiation, viscous dissipation, and thermo-diffusion and Dufour impacts. The flow is examined through an extending zone along with inconsistent thickness. The partial differential equations are extremely nonlinear and lessen to ODEs throughout of the appropriate similarity transformation. The system of nonlinear and coupled ODEs is handled applying a numerical approach with shooting procedure. Numerical solutions for momentum and energy descriptions are deliberated through graphs and tabular form for the impacts of magnetic parameter, Soret and Dufour variables, momentum power index variable, Schmidt number, wall thickness variable, without dimensions velocity slip, heat jump and mass jump variable. Outcomes illustrate that the momentum, temperature, and concentration transfer of the laminar boundary layers of equally non-Newtonian liquid motions are non-consistent. A comparison made with the existing literature which shows an good agreement and confidence of the present outcomes. It shows that Casson parameter restricted the skin friction, local heat and mass transfer while λ enhanced the skin friction, local heat and mass transfer. Velocity slip constant decreases the skin friction, local heat and mass transfer and a similar observation for thermal slip constant while an opposite phenomena for the solutal slip constant.

Keywords: Non-linear radiation; Viscous dissipation; MHD; Soret and Dufour effects; Cross-diffusion.

1. Introduction

The investigation in the flow field and heat transfer phenomena has established an immense compact of research attention due to its significant impact in the field of science and technology. One such study involves the energy and concentration transport over a variable thickness of the slender stretching sheet which highly momentous in the field of industries; namely petroleum industries for heat-treated materials, operating between rolls or on a conveyor belt, material production by extrusion processes, etc. Further, it helps in controlling the processes with outcomes. Ibrahim et al. [1] reported the combined convection on the magnetohydrodynamic motion of Casson liquid over a nonlinear extending sheet with a chemical reaction. Mustafa et al. [2] reviewed the laminar motion of nanoliquid past a non-linearly stretching sheet with the impact of Brownian and thermophoretic flow. Bhattacharyya et al. [3] reported the energy and concentration transport of viscous incompressible liquid past a shrinking sheet under the influence of Soret and Dufour impacts. The impact of Soret and Dufour impacts on the MHD motion of a Casson liquid past a stretching surface under the impression of changeable thermal conductivity was reported by Venkateswarlu and Satya Narayana [4]. Kumaran et al. [5] viewed the impact of the discontinuous heat source/sink of magnetohydrodynamic non-Newtonian liquids over an extending sheet with cross-diffusion. The influence of chemical reaction on the magnetohydrodynamic steady laminar motion of Williamson liquid past a permeable medium to a horizontal linearly extending surface has been surveyed by Krishnamurthy et al. [6]. Pushpalatha et al. [7] considered the MHD Casson liquid flow over a stretching sheet with the impression of cross-diffusion impact. The impact of radiation and discontinuous energy source of visco-elastic fluid motion past an extendable surface has been explored by Abel and Mahesha [8]. Hamid et al. [9] inspected the mixed effect of Ohmic heating on the motion of Williamson liquid over a permeable an extending sheet with internal friction. Sreedevi et al. [10] have reported the heat and mass diffusion liquid motion past a nonlinear extending sheet in the impression of radiative energy flux. Ajayi et al. [11] reviewed the impact of internal friction and dual stratification on Casson fluid motion past an extending surface with changeable thickness. Soomro et al. [12] have stated the transport of energy and concentration effect of melting transport of energy investigation of magnetohydrodynamic Sisko liquid past an extending surface under the impression of nonlinear thermal radiation. Aly [13] has studied the flow and transport of energy properties of 4sorts of nanoparticles (Ag, Cu, TiO_2, and Al_2O_3) within the foundation liquid (water) of laminar motion past a convective extending sheet under the impression of the normal magnetic field. Dogonchi and Ganji [14] have investigated the impact of the Brownian motion of Cu-H_2O and Al_2O_3-H_2O

Published online: April 02 2021

nanofluids past an extending sheet with thermal radiation. Besthapu et al. [15] took into consideration the magnetohydrodynamic stagnation end of the Casson nanofluid motion over an extending surface in the influence of slip impact. Soomro et al. [16] have employed the Prandtl nanofluid stagnation-point motion past an extending surface with the impact of convection boundary conditions. Akbar et al. [17] evaluated the channel motion problem of Williamson nanoliquid motion. Nadeem et al. [18] have explored the numerical evaluation of laminar motion and transport of energy of Oldroyd-B nanoliquid motion over an extending surface. Nadeem et al. [19] surveyed the Jefferey fluid over an extending surface in the presence of Brownian and thermophoresis flow. Priyadarsan and Panda [20] analyzed the flow and transport of energy examination of MHD second-grade liquid in a waterway with porous partition. Mohyud-Din et al. [21] have examined the investigation of transport of energy examination for the squeezing flow of a non-Newtonian fluid. Jayachandra and Sandeep[22] investigated diffusion thermo and thermo-diffusion impacts on magnetohydrodynamic non-Newtonian fluid motion past an extending sheet. They discussed the double outcomes that are exhibited for Newtonian liquid and non-Newtonian liquid and established that thermo-diffusion and diffusion thermo impacts float to manage the energy and mass boundary layers. Sulochana et al. [23] viewed the effect of the heat source and thermo-diffusion on the 2D MHD laminar motion of chemically reacting non-Newtonian liquid motion past an inclined permeable sheet. Sulochana et al. [24] have investigated the transfer of energy and concentration on a 3D MHD Newtonian and non-Newtonian fluid motion over an extending surface. The effect of diverse constraints on the transfer of heat and concentration of 2-D magnetohydrodynamic motion of a dissipation Maxwell nano liquid over an extended surface were scrutinized by Sulochana et al. [25]. The MHD stagnation-point motion of a Carreau nanoliquid past an extending surface has been scrutinized by Sulochana et al. [26]. Sulochana et al. [27] observed the effects of the Joule heating on the laminar motion of two-dimensional obligatory convective motion of an MHD nanofluid alongside a determinedly affecting parallel needle with frictional heating impact. Sulochana et al. [28] have viewed the motion, transfer of energy, and concentration behavior of magnetohydrodynamic motion over a perpendicular revolving cone in permeable media with Brownian motion and thermophoresis impacts. Khader and Megahed [29] have investigated the numerical result for boundary layer motion because of a nonlinearly extending surface under the influence of variable thickness and slip velocity. For additional readings, researchers are referred to the articles [30–52]. Sheikholeslami et al. [53] have discussed the heat transfer phenomena for the nanofluid flow over for helical turbulator. An application of the nanofluid flow on the solar collector with turbulator has discussed by Sheikholeslami et al. [54]. Narendra et al. [55] have discussed the have discussed 3D MHD Casson nanofluid flow over a stretching sheet in the presence of viscous dissipation, chemical reaction and heat source / sink. Impact of heat generation / absorption for a Oldroyd B fluid by a inclined stretching sheet has been discussed by Mabood et al. [56]. Shoaib et al. [57] have discussed the hybrid nanofluid flow over the stretching sheer in the presence of thermal radiation. Here some more worked in these direction where researchers worked on fluid flow over stretching sheet [58-60].

In every part of the over studies, the authors paying attention to examining the transfer of the energy and mass of nature of the magnetohydrodynamic motion by taking into consideration one non-Newtonian fluid. In this investigation, the thermal and concentration transfer of two dimensional magnetohydrodynamic non-Newtonian liquid motions under the force of Soret and Dufour impacts are examined theoretically. The motion is alongside an extending field by variable thickness. The differential equations clarification the motion condition has been changed with the help of suitable transforms. Explanation of the problem is attained through enchanting the put on of shooting technique. From the result, it is supposed that the motion is concerned with various substantial properties. The impacts of individuals constraints on the motion and energy transfer are discussed by graphical and tabular outcomes.

2. Mathematical Formulation

Suppose the 2-D boundary layer MHD motion of non-Newtonian fluids motion over a stretched sheet under the influence of variable thickness. At this point, the x-axis is measured alongside the surface flow and the y-axis be vertical to it. It is hypothetical that $y = A(x+b)^{0.5(1-m)}$, $u_w(x) = U_0(x+b)^m$, $v_w = 0$, $m \neq 1$. This investigation does not take into account the induced magnetic field. An oblique magnetic field of strengthB_0 is employed as drawn in Fig. 1.

The rheological equation of the Casson liquid(Mukhopadhyay et al. (53))has been considered as follows:

$$\tau_{ij} = \begin{cases} 2\left(\mu_B + p_y(2\pi)^{-0.5}\right)e_{ij}, & \pi > \pi_c, \\ 2\left(\mu_B + p_y(2\pi_c)^{-0.5}\right)e_{ij}, & \pi < \pi_c, \end{cases}$$

where $\pi = e_{ij}e_{ij}$ is the product of the components of the deformation rate itself with the (i,j) components of the deformation rate (e_{ij}). The critical value of the π is defined by π_c. μ_B and p_y are the respective plastic dynamics viscosity and yield stress of the non-Newtonian Casson fluid.

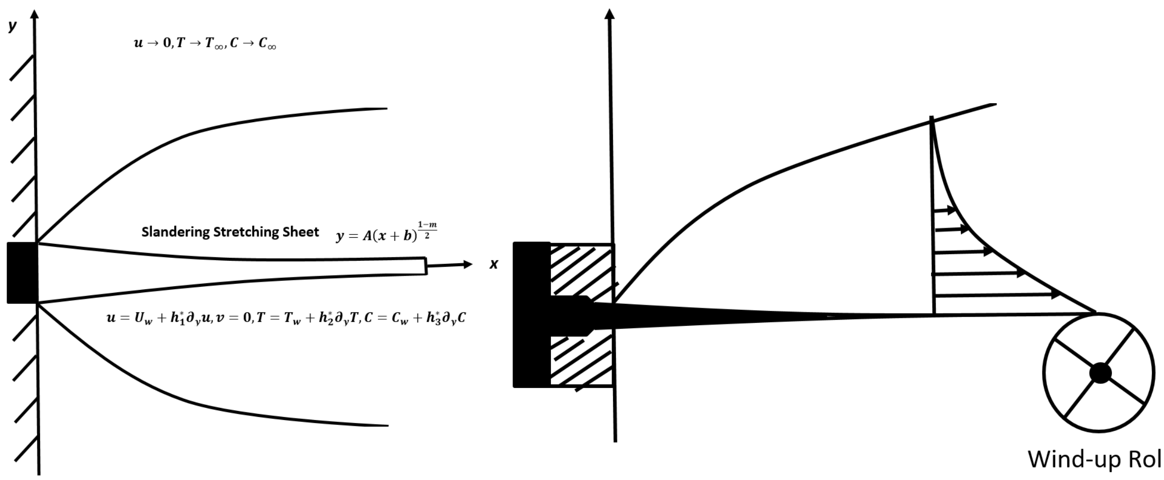

Fig. 1. Schematic diagram of the problem with engineering application in wind-up roll

Under the over conditions, the governing conservation equations for the steady 2-D motion of a Casson and Williamson liquids are as follows:

$$\partial_x u + \partial_y v = 0, \tag{1}$$

$$u\partial_x u + v\partial_y u = \nu\left(1+\beta^{-1}\right)\partial_{yy}u - \sqrt{2}\nu\Gamma\partial_y u\partial_{yy}u - \rho^{-1}\sigma B^2(x)u, \tag{2}$$

$$u\partial_x T + v\partial_y T = \kappa/\rho C_p\,\partial_{yy}T + D_m k_T/C_s C_p\,\partial_{yy}C + 1/\rho C_p\,\partial_y q_r + \mu/\rho C_p\left(\partial_y u\right)^{-1} \tag{3}$$

$$u\partial_x C + v\partial_y C = D_m\partial_{yy}C + D_m k_T/T_m\,\partial_{yy}T, \tag{4}$$

Eqs. (1)–(4) are subject to the following initial and boundary conditions

$$\left.\begin{array}{l} u(x,y)=0, T(x,y)=0, C(x,y)=0 \text{ for } t=0 \\ u(x,y)=U_w(x)+h_1^*\left(\partial_y u\right), v(x,y)=0, \\ T(x,y)=T_w(x)+h_2^*\left(\partial_y T\right), C(x,y)=C_w(x)+h_3^*\left(\partial_y C\right) \\ u=0,\ T=T_\infty\ , C=C_\infty\ at\ y=\infty \end{array}\right\} \tag{5}$$

where

$$h_1^* = (2-f_1)f_1^{-1}\xi_1(x+b)^{0.5(1-m)},\ \xi_2=(2\gamma)(1+\gamma)^{-1}\frac{\xi_1}{\Pr}, \tag{6}$$

$$h_2^* = (2-a)a^{-1}x_2(x+b)^{0.5(1-m)}, x_3=(2g)(1+g)^{-1}\frac{x_2}{\Pr}, \tag{7}$$

$$h_3^* = (2-d)d^{-1}\xi_3(x+b)^{0.5(1-m)},\ B(x)=B_0(x+b)^{0.5(m-1)}, \tag{8}$$

$$T_w(x)=T_\infty+T_0(x+b)^{0.5(1-m)} \text{ and } C_w(x)=C_\infty+C_0(x+b)^{0.5(1-m)} \tag{9}$$

Using the Rosseland approximation, we obtain

$$q_r = -4\sigma^* / 3k^*\partial_y T^4 = -16\sigma^* / 3k^* T^3\partial_y T \tag{10}$$

where σ^* the Stefan-Boltzman constant and k^* mean absorption coefficient. Now we propose the subsequent similarity transformations:

$$\psi(x,y)=f(\eta)\left(2/(m+1)\nu U_0(x+b)^{m+1}\right)^{0.5} \tag{11}$$

$$\eta = y\left((m+1)/2U_0(x+b)^{m-1}/\nu\right)^{0.5}, \tag{12}$$

$$\theta=(T_w(x)-T_\infty)/T-T_\infty \text{ and } \phi=(C_w(x)-C_\infty)/C-C_\infty. \tag{13}$$

which gives the velocities as

$$u=U_0(x+b)^m f'(\eta) \text{ and } v=-\left((m+1)/2\right)^{-1}\left(\nu U_0(x+b)^{m-1}\right)^{-1}\left(f'(\eta)\,\eta(m-1/m+1)+f(\eta)\right) \tag{14}$$

where ψ is the stream function which is defined in the classical form as $u=\partial_y\psi$ and $v=-\partial_x\psi$.

Using Eqs. (11), (12), (13) and (14), Eqs. (2) - (5) changed as

$$\left(1+\beta^{-1}\right)f''' + f''f - 2m/m+1\,f'^2 + \Lambda f''f''' - Mf' = 0, \tag{15}$$

$$\left(1+4/3R\left(1+(\theta_w-1)\theta\right)^3\right)\theta'' + 4R(\theta_w-1)\left(1+(\theta_w-1)\theta\right)^2\theta'^2 - \Pr(1-m)/(m+1)f'\theta + \mathrm{Ec}\Pr f''^2 + \Pr f\theta' + \Pr Du\,\phi'' = 0, \tag{16}$$

$$\phi'' - Sc(1-m)/(m+1)f'\phi + Scf\phi' + ScSr\,\theta'' = 0, \tag{17}$$

The corresponding initial and boundary conditions are

$$\left.\begin{array}{l} f'(\eta)=0,\ \theta(0)=0,\ \phi(0)=0 \text{ for } t=0 \\ f(0)=\lambda(1-m/1+m)(1+h_1f''(0)),\ f'(0)=(1+h_1f''(0)), \\ \theta(0)=(1+h_2\theta'(0)),\ \phi(0)=(1+h_3\phi'(0)), \\ f'(\infty)=0,\ \theta(\infty)=0,\ \phi(\infty)=0, \end{array}\right\} \tag{18}$$

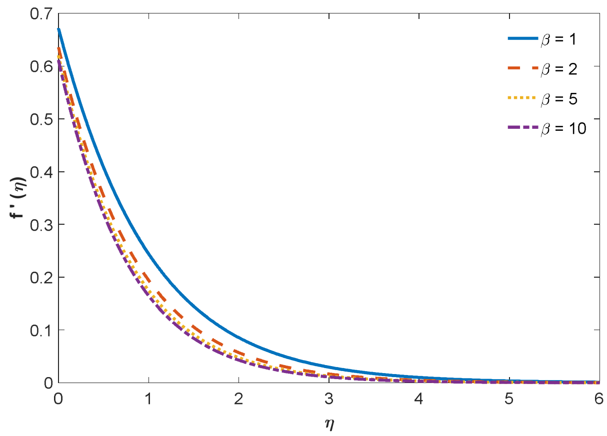

Fig. 2. Velocity field for diverse Casson parameter β

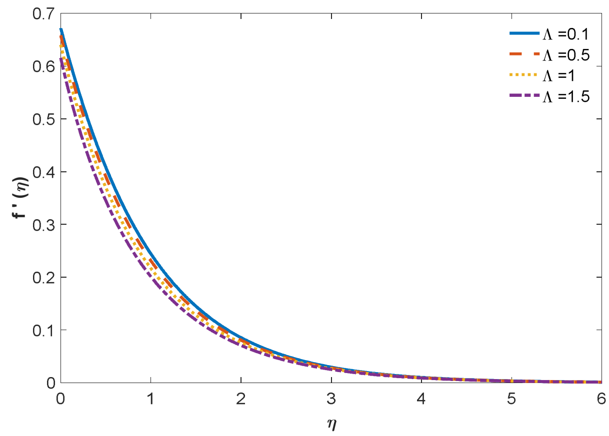

Fig. 3. Velocity field for diverse Williamson parameter Λ

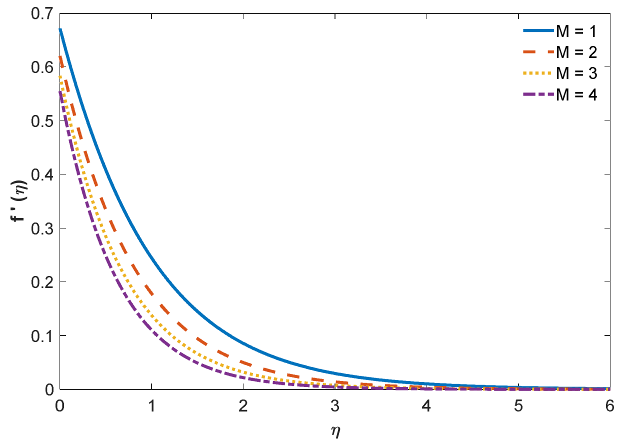

Fig. 4. Velocity field for diverse magnetic parameter M

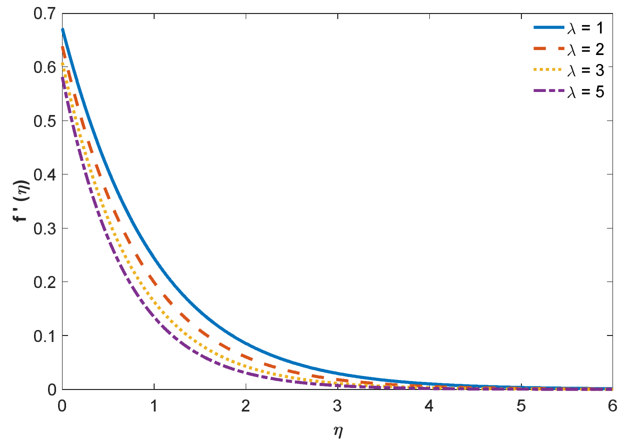

Fig. 5. Velocity field for diverse slip velocity parameter λ

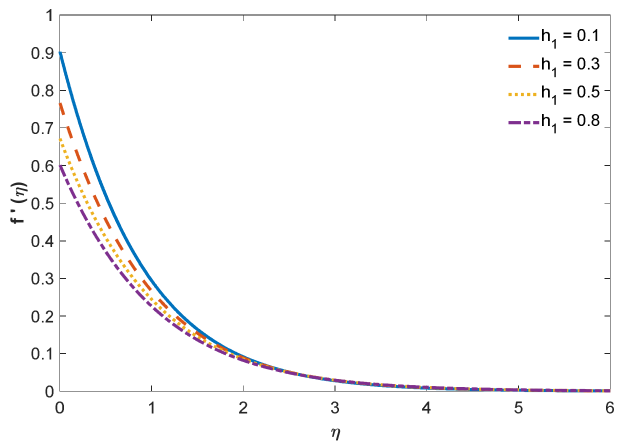

Fig. 6. Velocity field for diverse slip velocity parameter h_1

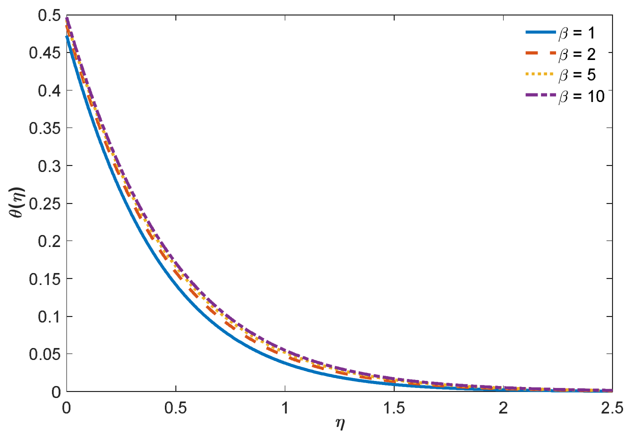

Fig. 7. Temperature field for diverse Casson variable β

where Λ, M, $\Pr$, Du, Sc, Sr are elucidated as

$$\left.\begin{array}{l} \Lambda = \Gamma\left((m+1)U_0^3(x+b)^{3m-1}/\nu\right)^{0.5}, \\ M = 2\sigma B_0^2/\rho U_0(m+1),\ \Pr = \mu C_p/\kappa,\ Du = D_m k_T(C_w - C_\infty)/\nu C_s C_p(T_w - T_\infty),\ \theta_w = T_w/T_\infty, \\ Ec = U_w^2/C_p(T_w - T_\infty),\ Sc = \nu/D_m,\ Sr = D_m k_T(T_w - T_\infty)/\nu T_m(C_w - C_\infty),\ R = 4\sigma^* T_\infty^3/\kappa k^*. \end{array}\right\} \tag{19}$$

The substantial quantities of importance, the resistance factor, transfer of heat and mass rate coefficients are specified as

$$C_f = 2\mu\partial_y u/\rho U_w^2,\ Nu_x = (x+b)\partial_y T/T_w(x) - T_\infty,\ Sh_x = (x+d)\partial_y C/C_w(x) - C_\infty \tag{20}$$

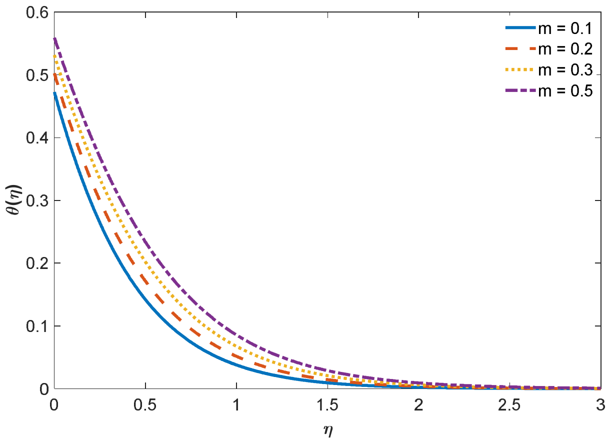

Fig. 8. Temperature field for diverse values of m

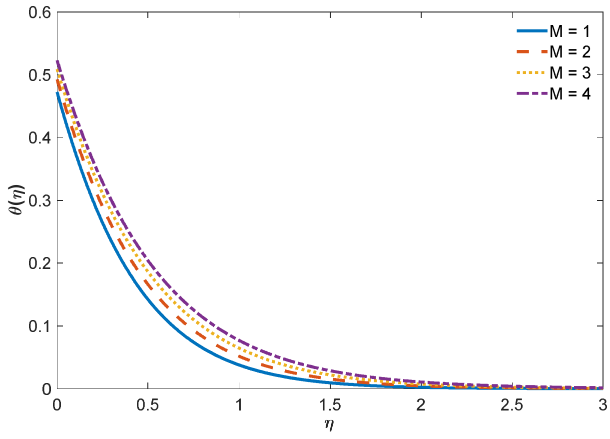

Fig. 9. Temperature description for diverse magnetic variable M

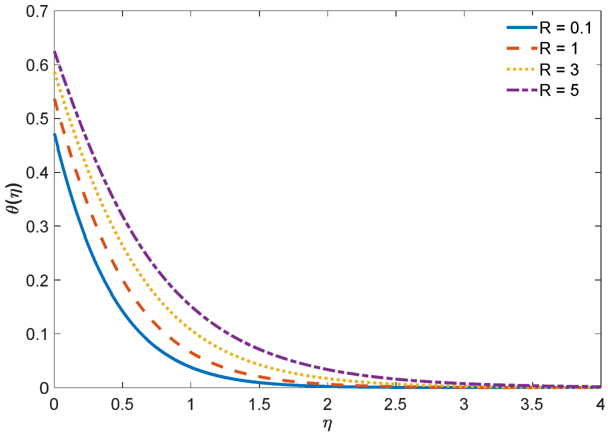

Fig. 10. Temperature field for diverse values of radiation variable R

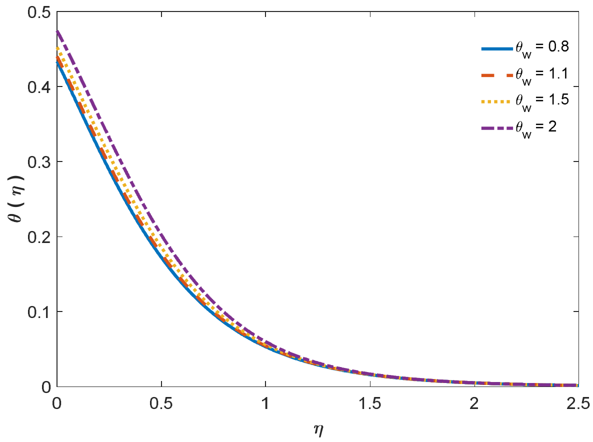

Fig. 11. Impact of energy ration θ_w on temperature field

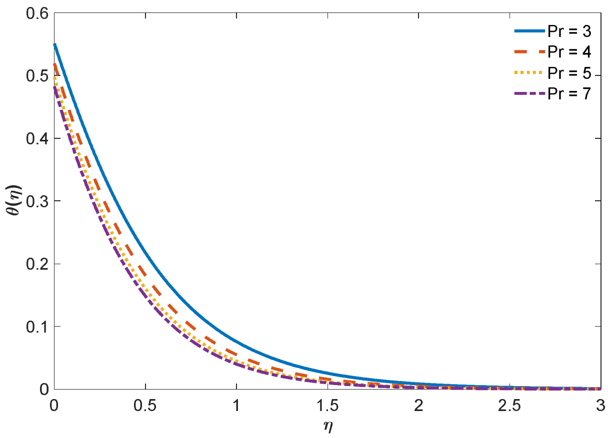

Fig. 12. Energy field for diverse Prandtl number Pr

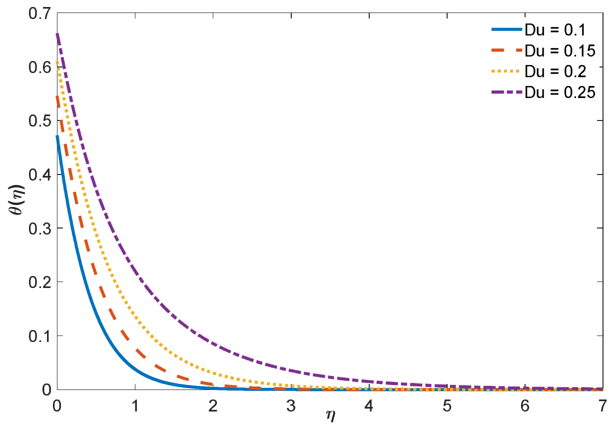

Fig. 13. Temperature field for diverse Dufour parameter Du

By employing (5), Eq. (20) becomes

$$\left.\begin{aligned} &C_f\,(\mathrm{Re}_x)^{0.5} = 2(m+1/2)^{0.5}\left(\left(1+\beta^{-1}\right)f''(0)+\Lambda f''^2(0)\right), \\ &Nu_x = -(m+1/2)^{0.5}(\mathrm{Re}_x)^{0.5}\left(1+4/3\,\mathrm{R}\left(1+(\theta_w-1)\theta\right)^3\right)\theta'(0), \\ &\mathrm{Sh}_x = -(m+1/2)^{0.5}(\mathrm{Re}_x)^{0.5}\,\phi'(0), \end{aligned}\right\} \tag{21}$$

where $\mathrm{Re}_x = U_w X/\nu$ and $X = (x+b)$.

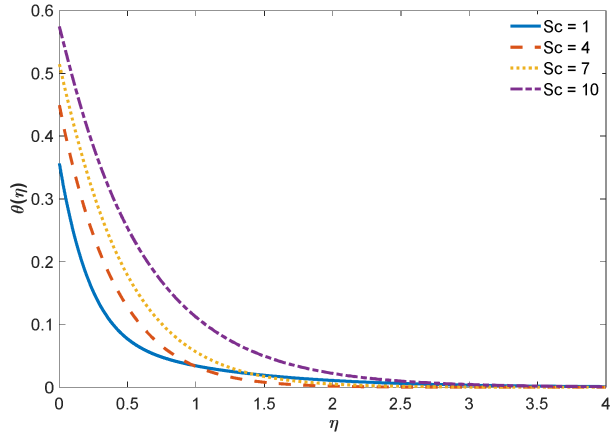

Fig. 14. Temperature field for diverse Schmidt number Sc

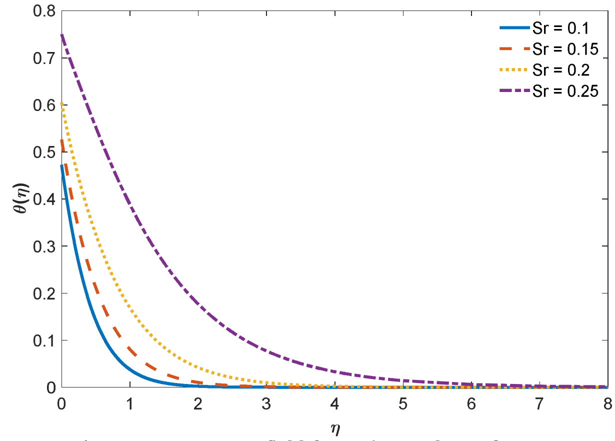

Fig. 15. Temperature field for various values of Sr

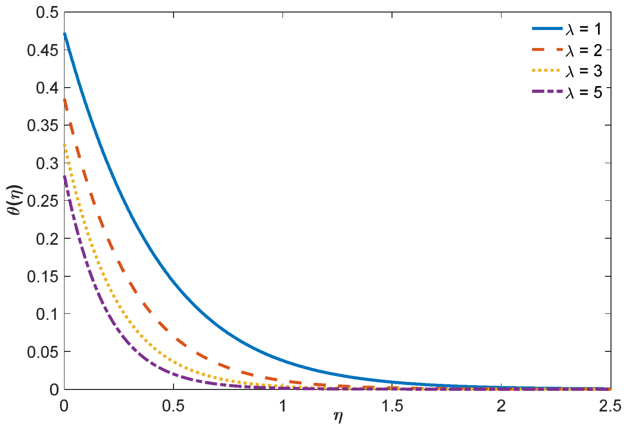

Fig. 16. Energy description for various values of λ

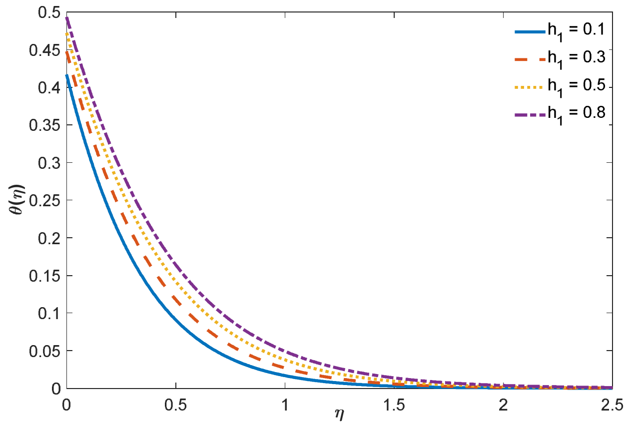

Fig. 17. Energy description for various values of velocity slip variable h_1

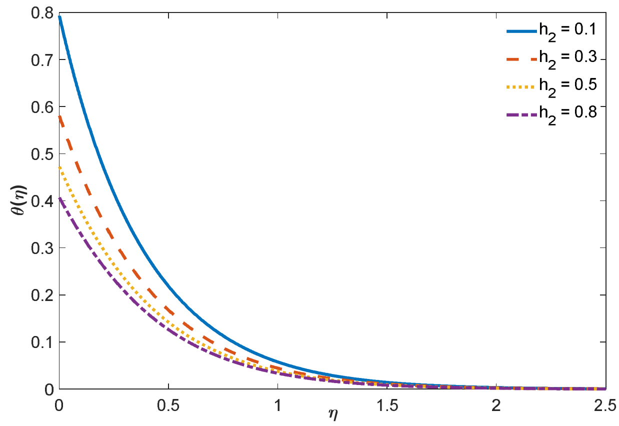

Fig. 18. Energy description for diverse values of temperature slip var. h_2

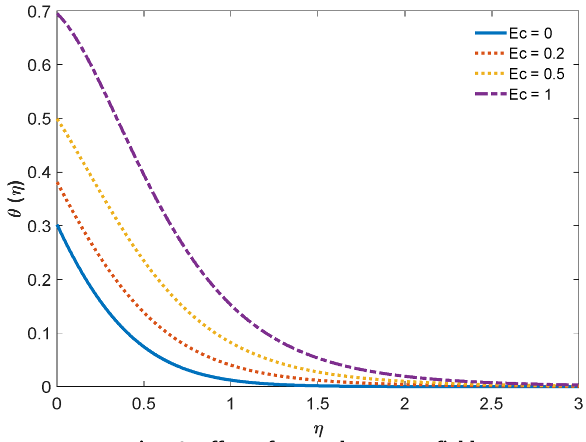

Fig. 19. Effect of Ec on the energy field

3. Results and Discussion

The system of governing equations are highly coupled and non-linear. The governing equations (15)-(17) with the boundary condition (18) are resolved numerically by applying the bvp4c routine of MATLAB which based on the 4th-order Range-Kutta technique with shooting techniques. We had equated our outcomes with existing literature of Mabood et al. [61] and Khan et al. [62] under certain constraints and have observed a good approximation with that literature (see Table 1). This comparison gives us confidence in further results. The general values of the parameters as $\beta = 1$, $m = 0.1$, $\Lambda = 0.1$, $M = 1$, $R = 0.1$, $\Pr = 7$, $Du = 0.1$, $Sc = 5$, $Sr = 0.1$, $\lambda = 1$, $h_1 = h_2 = h_3 = 0.5$ are considered in the present analysis. The velocity profile for the different parameters is illustrative in Figs. 2-6. Figs. 2 and 3 are outlined for velocity distribution against the Casson fluid variable (β) and Williamson liquid parameter (Λ) .It is noted that by enhancing the values of the Casson fluid parameter (β) and Williamson liquid parameter (Λ) the magnitude of the momentum inclines to decrease. Higher Casson parameter implies the absence of the yield stress which approaches the Newtonian nature of the fluid. The influence of the M on the dispersal of momentum is exposed in Fig. 4.

Table 1. Comparison of $-\theta'(0)$ with Mabood et al. [62] and Khan et al. [57] for $\beta \to \infty, m = 1,\ \Lambda = M = R = Ec = Du = Sr = h_1 = h_2 = h_3 = 0$.

Pr	Mabood et al. [62]	Khan et al. [63]	Current Outcomes
0.07	0.0665	0.0645	0.06449271
0.2	0.1691	0.1663	0.16631332
0.7	0.4539	0.4554	0.45540012
2	0.9114	0.9100	0.91102381
7	1.8954	1.8929	1.89432002
20	3.3539	3.3505	3.35045413
70	6.4622	6.4598	6.46010020

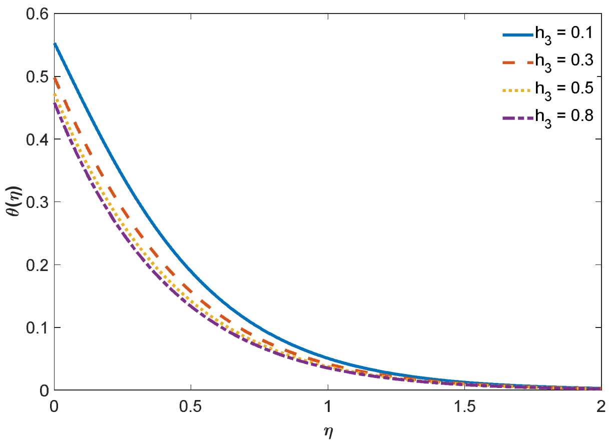

Fig. 20. Temperature profile for diverse values of concentration slip parameter h_3

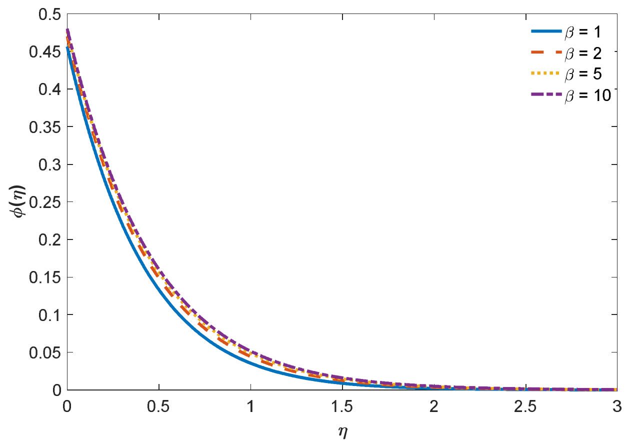

Fig. 21. Mass profile for diverse Casson parameter β

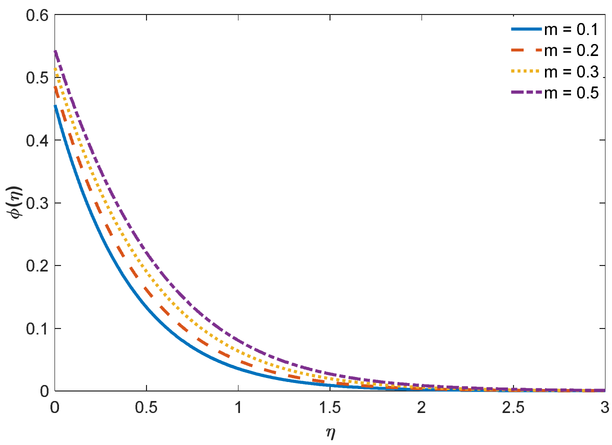

Fig. 22. Mass field for various values of m

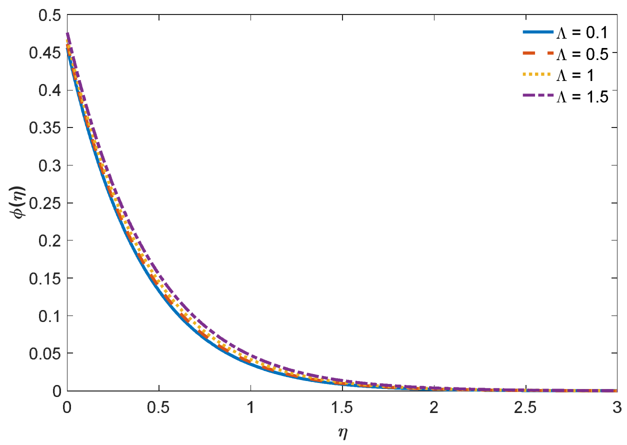

Fig. 23. Mass field for various values of Williamson number Λ

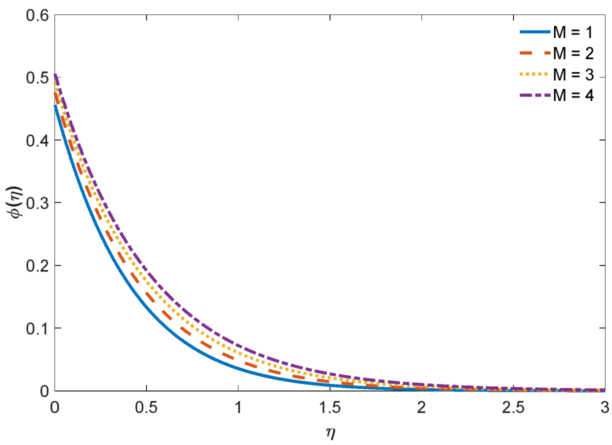

Fig. 24. Maas profile for diverse magnetic number M

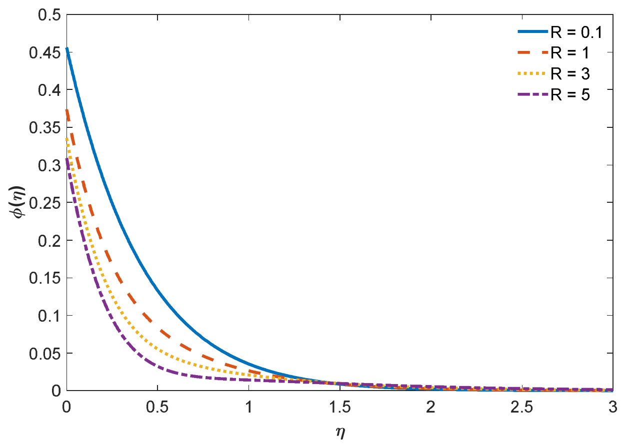

Fig. 25. Mass profile for diverse values of radiation parameter R

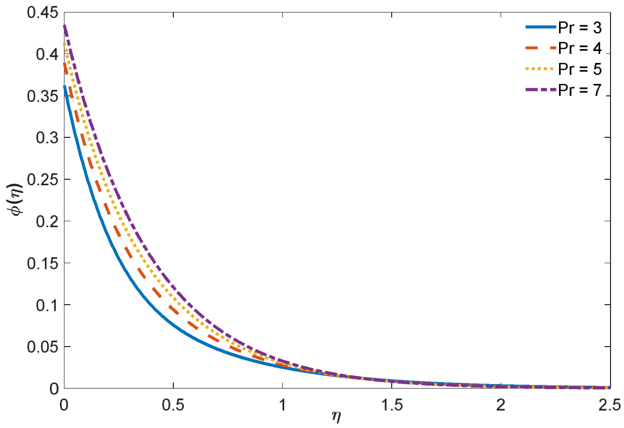

Fig. 26. Mass profile for diverse values of Prandtl number Pr

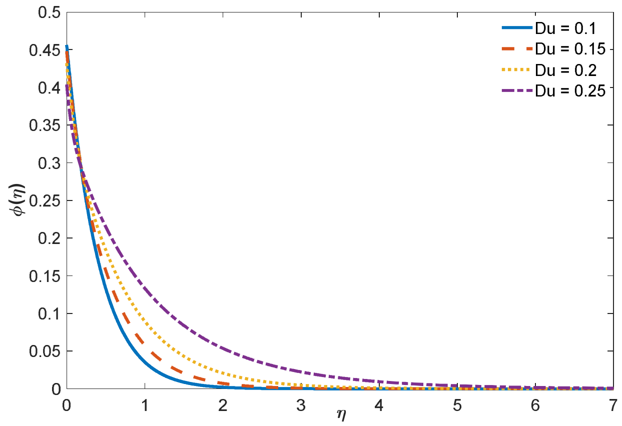

Fig. 27. Mass profile for diverse values of Du

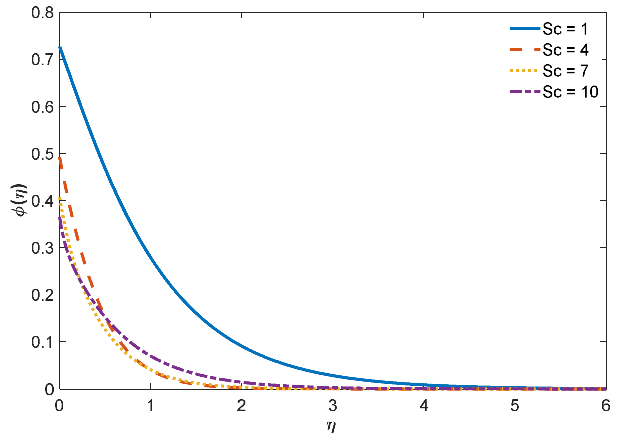

Fig. 28. Mass field for diverse values of Sc

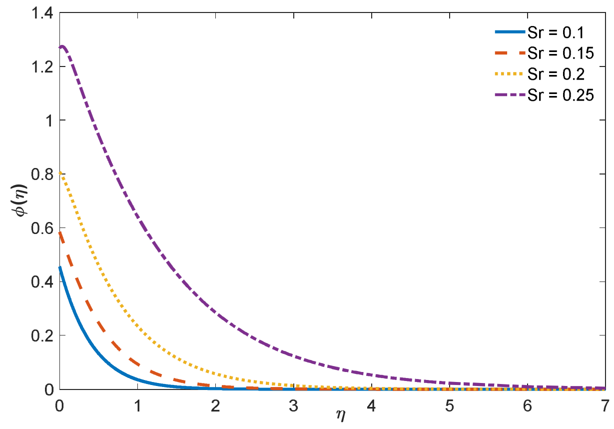

Fig. 29. Mass field for diverse values of Sr

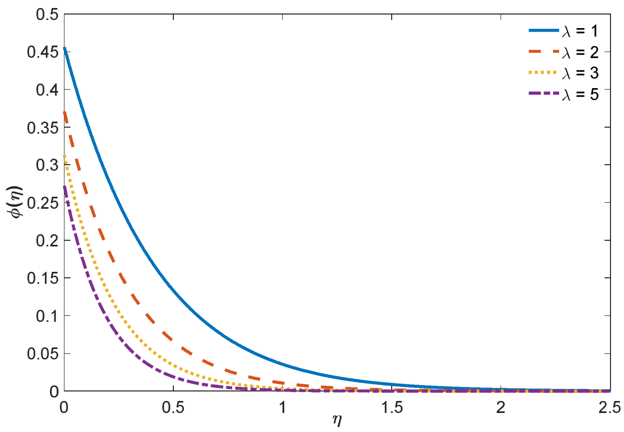

Fig. 30. Mass profile for diverse values of λ

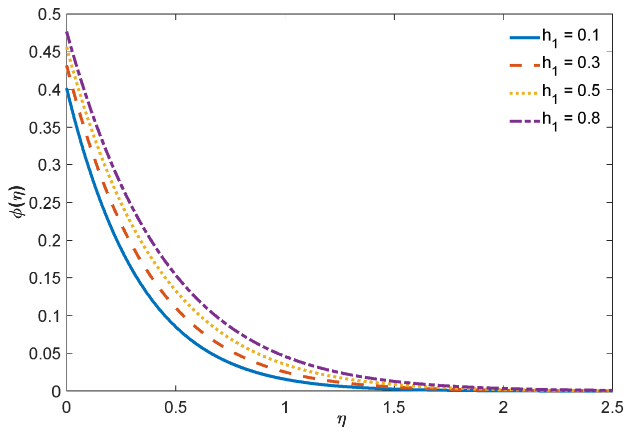

Fig. 31. Mass field for various values of velocity slip variable h_1

It is noted that the upsurge in the (M) decreases the distribution of momentum. An increase in the (M) yields a resisting nature of force named Lorentz force is produced in the motion which roots a reduction in causes of momentum description particles and subsequently, the momentum of the liquid decreases. Fig. 5 displays the impact of the wall thickness variable (λ) on the momentum description. By enhancing the values of λ, the consistent velocity boundary layer thickness and momentum reduced. This happens because extending momentum is partially transforming the trouble frictional relationship between the sheet and the fluid. Fig. 6 is elucidating the impact of the slip momentum parameter on the momentum description. It is noticeable that arising value h_1 reduces the velocity description. It is too detected that the enhancing value of the h_1 decreases the velocity boundary layer thickness. We detected that the rise in Casson liquid variable (β) increases the temperature field (Fig. 7). This happens because the escalation in Casson liquid parameter (β) enhances the viscous forces, and these forces produce some heat energy in the motion. Therefore, the dispersal of energy increases by huge β. The effect of the velocity power parameter m on energy distribution $\theta(\eta)$ is publicized in Fig. 8. It is remarked that an enhancing value of the momentum power parameter (m) elevates the temperature profiles.

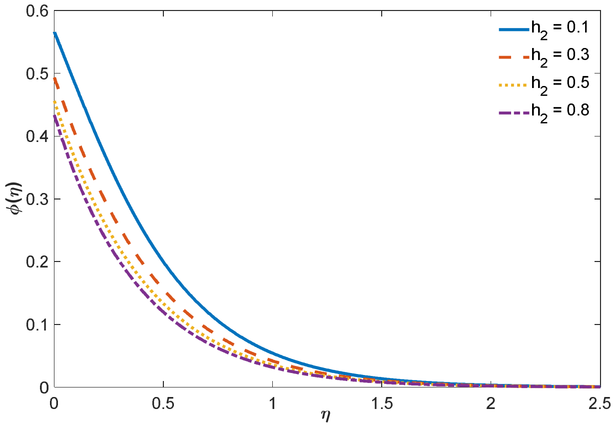

Fig. 32. Mass field for diverse values of temperature slip variable h_2

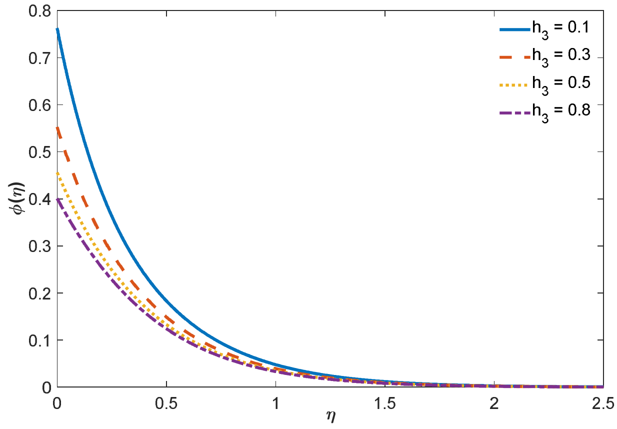

Fig. 33. Mass profile for diverse values of concentration slip variable h_3

Fig. 9 reveals the stimulus of the magnetic parameter on the energy field. It is noted that raising the value of the magnetic variable enhances the energy of the liquid. The stimulus of R on the dispersal of the energy field is revealed in Fig. 10. We observe that the enhance in radiation parameter (R) enhances the liquid energy description. The rise in radiation parameter discharges temperature to the motion so this heat assists to admire the energy description. Fig. 11 illustrates the impact of the heat ratio parameter on the energy field. It is noted that an enhance in the heat profile with enhancing values of energy ratio parameter was noticed. The variations in the energy $\theta(\eta)$ field are established with the Prandtl number (Pr) via Fig. 12. It is observed that enhancing the values of Pr lessens the energy field. It is detected that the larger effect of Pr, energy distribution reduces a raise in Prandtl number associated with the weedier current diffusivity contain temperature.

Fig. 13 displayed the stimulus of the Dufour parameter on the energy field. It is evident that the rising values of Dufour parameter (Du)increasing the heat description. Substantially, the Dufour impact takes place in the energy equation regulates the role of thermal temperature reduced through the mass gradients in the motion. This increases the liquid momentum and stretches an increase to the thermal temperature to the motion.

Fig. 14 depicts the influence of Sc on the temperature field. An upsurge in the energy profile with an increasing value of the Schmidt number (Sc) has been observed. Fig. 15 elucidates the effect of the Soret number (Sr) on the energy field. It is seen that the energy description increase with the enhances of Sr.

The discrepancy of energy for diverse values of the wall thickness parameter (λ) is presented in Fig. 16. In enhancing the values of the λ boundary layer converts heavier. As a result of a notable rise in energy, we observed that energy is enhancing λ.

The impacts of momentum and temperature slip parameter in Figs. 17-18. It is explicitly that enhancing the value of h_1 enhances the energy boundary layer width. Nevertheless, we noted an opposite tendency for enhancing the values of the h_2. Fig. 19 shows the discrepancy of the Ec on the temperature description. For minor Ec, the term in the temperature equation describing the pressure changes and body force in heat can be neglected. Therefore, energy distribution enhances with an enhance in the Eckert number.

The impact of the concentration slip variable h_3 on the energy description is seen in Fig. 20. It is noted that enhancing the value of h_3 reducing the energy description. Fig. 21 elucidates the impact of the Casson parameter (β) on the mass field. An upsurge in the mass field with enhancing the values of the (β) has been noticed. The impact of the momentum power parameter on the mass description has been depicted in Fig. 22. An upsurge in the mass profile with enhancing values of m has been observed.

Table 2. Variation in $C_{fx}, -\theta'(0)$ and $-\phi'(0)$ for various parameters for Casson-Williamson fluid.

β	Λ	M	λ	h_1	h_2	h_3	$\frac{C_{fx}}{\sqrt{Re_x}}$	$\sqrt{Re_x}\,Nu_x$	$\sqrt{Re_x}\,Sh_x$
1	0.1	1	1	0.1	0.1	0.1	-1.91442223	0.88655164	0.80637031
2							-1.58152215	0.86268862	0.78579417
5							-1.35621023	0.84147804	0.76748970
10							-1.27541797	0.83249053	0.75972876
	0.5						-1.83996805	0.88007212	0.80077821
	1						-1.73472880	0.86985819	0.79195697
	1.5						-1.60878618	0.85566507	0.77968510
		2					-2.20857094	0.85231598	0.77683993
		3					-2.41807186	0.82486720	0.75313668
		4					-2.58062546	0.80153137	0.73296352
			2				-2.10641535	1.03369620	0.93316707
			3				-2.27886286	1.13395467	1.01892869
			5				-2.56882510	1.25637672	1.12326615
				0.3			-2.26626363	0.92816767	0.84235742
				0.5			-1.91442192	0.88655168	0.80637035
				0.8			-1.56499203	0.83580394	0.76235387
					0.3		-1.91442192	1.17408590	0.75133875
					0.5		-1.91442192	0.88655168	0.80637035
					0.8		-1.91442192	0.64837180	0.85195594
						0.3	-1.91442192	0.84402452	1.10550035
						0.5	-1.91442192	0.88655168	0.80637035
						0.8	-1.91442192	0.91964852	0.57357185

Fig. 23 reveals the effect of the Λ on the mass field. It is seen that the mass field enhances as rising the Williamson parameter (Λ). The influence of the M on the mass description is illustrated in Fig. 24. The energy field increases with an upsurge in the M while in the case of the radiation parameter, the reverse effect is observed (Fig. 25).

Fig. 26 displayed the impact of Pr on the mass field. It is noted that the mass boundary layer width is enhanced as the value of the Pr rises. Since the Pr is the proportion of the kinematic viscosity to current diffusivity. Hence, for larger values of Pr liquid converts extra viscous and transfers gradually because of near interface particle form, thus concentration boundary layer width is augmented.

Fig. 27 depicts that an enhance in the Dufour number, enhances the concentration field. Fig. 28 explains the influence of Sc on the concentration field $\varphi(\eta)$. We detected that the mass field $\varphi(\eta)$ is a reducing function of the Schmidt number. This is because of the rate of concentration diffusivity is contrary wise proportionate to Sc. The Sc appears straight in the mass equation. The mass boundary layer width reduces over enhance in Sc. Fig. 29 elucidates the influence of Sron $\varphi(\eta)$. It is observed that an enhance in the Sr exhibits a rise in the $\varphi(\eta)$.

The impact of the λ on the mass description is explored in Fig. 30. It is noticed that the augmenting value λ reduces the mass boundary layer of the fluid. Figs. 31-33 are illuminating the influence of slip parameter h_1, h_2 and h_3 on the mass field. Fig. 31 displays the influence of the velocity jump parameter on the mass field. It is remarked that the mass field increase as the velocity jump parameter rises while the reverse effect observed for temperature and concentration slip parameter (Fig. 32 and Fig. 33).

Table 2 reveals the influence of pertinent parameters on the wall friction rate of heat and mass transport in Casson and Williamson motions. The enhancing value of the Casson parameter increases skin friction as it rises the yield stress. Casson parameter increased the energy near to the sheet and hence it lessens the local energy and concentration transfer rate. The skin friction upsurges with the increase with the Williamson number. Skin friction is higher in the absence of Williamson fluid nature. As the Casson parameter, enhanced in Williamson number reduces the energy and concentration transfer rate. A higher magnetic field rises the skin friction while the temperature and concentration transfer rate decreases. This is because the Lorentz force act on the system. The skin friction rises with an upsurge in the λ and a similar phenomenon observed for the temperature and concentration transfer rate. $h_1$significantly decreases the skin friction but no impact with an increase of h_2 and h_3. All $h_i(i = 1, 2, 3)$ are significant for the temperature and concentration transfer rate on the surface.

4. Conclusions

In the current investigation, the temperature and concentration transport for the Casson and Williamson liquid motions is considered. The motion is through an extending sheet of variable thickness. The solution to the problem is found using the shooting method. The present problem compare with the existing literature which shows a good agreement. The major outcomes of the review are like follows briefly:

- Lorentz force influences Williamson fluid flow much more as differentiate to the Casson liquid motion.
- The energy, concentration and velocity boundary layer are non-uniform for both the Casson and Williamson fluid flows.
- Energy and mass transfer rates are excessive for Casson's motion as compared to Williamson's motion.
- Williamson number enhanced the velocity, while reduced the solutal boundary layer thickness. It is further restricted the local heat and mas transfer rate.
- Velocity slip (h_1) decreases the skin friction along with the Nusselt and Sherwood number.
- The thickness of the sheet increases the energy and concentration transfer rate.
- The wall friction enhances with the enhance of velocity slip.
- Local Nusselt number and Sherwood number are regulated by temperature and concentration jump parameter.

Author Contributions

Ram Prakash Sharma worked on the abstract, introduction, and results and discussion part and Sachin Shaw worked on the numerical scheme and mathematical formulation part.

Acknowledgments

The author are very much thankful to the learned reviewers for their qualitative suggestions to improve the quality of our manuscript.

Conflict of Interest

The authors declared no potential conflicts of interest with respect to the research, authorship and publication of this article.

Funding

The authors received no financial support for the research, authorship and publication of this article.

Data Availability Statements

The datasets generated and/or analyzed during the current study are available from the corresponding author on reasonable request.

Nomenclature

A	Constant	f_1	Constant
b	Constant	a	Constant
B_0	Strength of the magnetic field	γ	Constant

π	Product of component of the deformation rate	d	constant
e_{ij}	Component of the deformation rate	ξ_1	Constant
π_c	Critical value of the deformation rate	ξ_2	Constant
μ_B	Plastic dynamics viscosity	ξ_3	Constant
p_y	Yield stress of the non-Newtonian Casson fluid	Pr	Prandtl number
(u, v)	Velocity components along respective x and y- directions	m	Constant
(x, y)	Coordinate system	σ^*	Stefan-Boltzmann constant
β	Casson number	k^*	Mean absorption coefficient
ν	Dynamics viscosity	U_0	Constant velocity
Γ	Williamson parameter	Λ	Surface velocity
Λ	Electrical conductivity	M	Magnetic number
κ	Thermal conductivity of the fluid	R	Radiation number
D_m	Diffusion coefficient	θ_w	Temperature ratio
k_T	Thermal-diffusion ratio	Ec	Eckart number
C_s	Concentration susceptibility	Du	Dufour number
C_p	Specific heat	Sc	Schmidt number
T_m	Mean temperature	Sr	Soret number
U_m	Mean velocity	λ	Constants
T_w	Temperature at the wall	C_f	Skin friction
C_w	Concentration at the wall	Nu_x	Nusselt number
T_∞	Ambient temperature	Sh_x	Sherwood number
C_∞	Ambient concentration		

References

[1] Ibrahim, S.M., Lorenzini, G., Vijaya Kumar, P., Raju, C.S.K., Influence of chemical reaction and heat source on dissipative MHD mixed convection flow of a Casson nanofluid over a nonlinear permeable stretching sheet, *International Journal of Heat and Mass Transfer*, 111, 2017, 346-355.
[2] Mustafa, M., Khan, J.A., Hayat, T., Alsaedi, A., Analytical and numerical solutions for the axisymmetric flow of nanofluid due to non-linearly stretching sheet, *International Journal of Non-Linear Mechanics*, 71, 2015, 22-29.
[3] Bhattacharyya, K., Layek, G.C., Seth, G.S., Soret and Dufour effects on convective heat and mass transfer in the stagnation-point flow towards a shrinking surface, *Physica Scripta*, 89(9), 2014, 1-15.
[4] Venkateswarlu, B., Satya Narayana, P.V., Influence of variable thermal conductivity on MHD Casson fluid flow over a stretching sheet with viscous dissipation, Soret and Dufour effects, *Frontiers in Heat and Mass Transfer*, 7(1), 2016, 1-16.
[5] Kumaran, G., Sandeep, N., Ali, N.E., Computational analysis of magnetohydrodynamic Casson and Maxwell flow over a stretching sheet with cross-diffusion, *Results in Physics*, 7, 2017, 147–155.
[6] Krishnamurthy, M.R., Prasannakumara, B.C., Gireesha, B.J., Gorla, R.S.R., Effect of chemical reaction on MHD boundary layer flow and melting heat transfer of Williamson nanofluid in a porous medium, *Engineering Science and Technology, an International Journal*, 19, 2016, 53–61
[7] Pushpalatha, K., Ramana Reddy, J.V., Sugunamma, V., Sandeep, N., Numerical study of chemically reacting unsteady Casson fluid flow past a stretching surface with cross-diffusion and thermal radiation, *Open Eng.*, 7, 2017, 69–76.
[8] Abel, M.S., Mahesha, N., Heat transfer in MHD viscoelastic fluid flow over a stretching sheet with variable thermal conductivity, non-uniform heat source, and radiation, *Appl. Math. Model.*, 32, 2008, 965–1983.
[9] Hamid, A.H., Khan, M., Hafeez, A., Unsteady stagnation-point flow of Williamson fluid generated by stretching/shrinking sheet with Ohmic heating, *International Journal of Heat and Mass Transfer*, 126, 2018, 933–940.
[10] Sreedevi, P., Reddy, P.S., Chamkha, A.J., Heat and mass transfer analysis of nanofluid over linear and non-linear stretching surfaces with thermal radiation and chemical reaction, *Powder Technol.*, 315, 2017, 94–204.
[11] Ajayi, T.M., Omowaye, A.J., Animasaun, I.L., Effects of viscous dissipation, and double stratification on MHD Casson fluid flow over a surface with variable thickness: boundary layer analysis, *Int. J. Eng. Res. Africa*, 28, 2017, 73–79.
[12] Soomro, F.A., Usman, M., U Haq, R., Wang, W., Melting heat transfer analysis of Sisko fluid over a moving surface with nonlinear thermal radiation via Collocation method, *International Journal of Heat and Mass Transfer*, 126, 2018, 1034–1042.
[13] Aly, E.H., Existence of the multiple exact solutions for nanofluid flow over a stretching/shrinking sheet embedded in a porous medium at the presence of a magnetic field with electrical conductivity and thermal radiation effects, *Powder Technol.*, 301, 2016, 760–781.
[14] Dogonchi, A.S., Ganji, D.D., Thermal radiation effect on the Nano-fluid buoyancy flow and heat transfer over a stretching sheet considering Brownian motion, *J. Mol. Liq.*, 223, 2016, 521–527.
[15] Besthapu, P., UlHaq, R., Bandari, S., Al-Mdallal, Q.M., Thermal radiation, and slip effects on MHD stagnation point of non-Newtonian nanofluid over a convective stretching surface, *Neural Comput. Appl.,* 31, 2019, 207-217.
[16] Soomro, F.A., Ul-Haq, R., Khan, Z.H., Zhang, Q., Passive control of nanoparticles due to convective heat transfer of Prandtl fluid model at the stretching surface, *Chin. J. Phys.*, 55, 2017, 1561–1568.
[17] Akbar, N.S., Nadeem, S., Lee, C., Khan, Z.H., Ul-Haq, R., Numerical study of Williamson nanofluid flow in an asymmetric channel, *Results Phys.*, 3, 2013, 161–166.
[18] Nadeem, S., Ul-Haq, R., Akbar, N.S., Lee, C., Khan, Z.H., Numerical study of boundary layer flow and heat transfer of Oldroyd-B nanofluid towards a stretching sheet, *PLoS One*, 8, 2013, 1-6.
[19] Nadeem, S., Ul-Haq, R., Khan, Z.H., Numerical solution of non-Newtonian nanofluid flow over a stretching sheet, *Applied Nanoscience*, 4, 2014, 625–631.
[20] Priyadarasan, K.P., Panda, S., Flow and heat transfer analysis of magnetohydrodynamic (MHD) second-grade fluid in a channel with the porous wall, *J. Br. Soc. Mech. Sci. Eng.*, 39, 2017, 2145–2157.
[21] Mohyud-Din, S.T., Usman, M., Wang, W., Hamid, M., A study of heat transfer analysis for squeezing flow of a Casson fluid via differential transform method, *Neural Computing and Applications*, 30, 2018, 3253–3264.
[22] Babu, M.J., Sandeep, N., MHD non-Newtonian fluid flow over a slandering stretching sheet in the presence of cross-diffusion effects, *Alexandria Engineering Journal*, 55, 2016, 2193–2201.
[23] Sulochana, C., AshwinKumar, G.P., Sandeep, N., Effect of frictional heating on mixed convection flow of chemically reacting radiative Casson nanofluid over an inclined porous plate, *Alexandria Engineering Journal*, 57, 2018, 2573-2584.
[24] Sulochana, C., AshwinKumar, G.P., Sandeep, N., Similarity solution of 3D Casson nanofluid flow over a stretching sheet with convective boundary conditions, *Journal of the Nigerian Mathematical Society*, 35, 2016, 128–141.
[25] Sulochana, C., AshwinKumar, G.P., Sandeep, N., Effect of Thermophoresis and Brownian moment on 2D MHD nanofluid flow over an elongated sheet, *Defect and Diffusion Forum*, 377, 2017, 111-126.
[26] Sulochana, C., AshwinKumar, G.P., Sandeep, N., Transpiration effect on the stagnation-point flow of a Carreau nanofluid in the presence of thermophoresis and Brownian motion, *Alexandria Engineering Journal*, 55, 2016, 1151–1157.
[27] Sulochana, C., AshwinKumar, G.P., Sandeep, N., Joule heating effect on a continuously moving thin needle in MHD Sakiadis flow with thermophoresis and Brownian moment, *Eur. Phys. J. Plus*, 132, 2017, 387.

[28] Sulochana, C., AshwinKumar, G.P., Sandeep, N., Numerical investigation of chemically reacting MHD flow due to a rotating cone with Thermophoresis and Brownian motion, *International Journal of Advanced Science and Technology*, 86, 2016, 61-74.
[29] Khader, M and Megahed, A.M., Numerical solution for boundary layer flow due to a nonlinearly stretching sheet with variable thickness and slip velocity, *The European Physical Journal Plus*, 128, 2013, 100-108.
[30] Shahzad, A., Ali, R., Approximate analytic solution for the magnetohydrodynamic flow of a non-Newtonian fluid over a vertical stretching sheet, *Can. J. Appl. Sci.*, 2, 2012, 202–215.
[31] Shahzad, A., Ali, R., MHD flow of a non-Newtonian power-law fluid over a vertical stretching sheet with the convective boundary condition, *Walailak J. Sci. Technol.*, 10, 2013, 43–56.
[32] Khan, M., Ali, R., Shahzad, A., MHD Falkner-Skan flow with mixed convection and convective boundary conditions, *Walailak J. Sci. Technol.*, 10, 2013, 517–529.
[33] Shahzad, A., Ali, R., Khan, M., On the exact solution for axisymmetric flow and heat transfer over a nonlinear radially stretching sheet, *Chin. Phys. Lett.*, 29, 2012, 084705.
[34] Rahimi-Gorji, M., Pourmehran, O., Gorji-Bandpy, M., Ganji, D.D., An analytical investigation on the unsteady motion of vertically falling spherical particles in a non-Newtonian fluid by collocation method, *Ain Shams Eng. J.*, 6, 2015, 531–540.
[35] Usman, M., Soomro, F.A., Ul-Haq, R., Wang, W., Defterli, O., Thermal and velocity slip effects on Casson nanofluid flow over an inclined permeable stretching cylinder via collocation method, *Int. J. Heat Mass Transf.*, 122, 2018, 1255–1263.
[36] Soomro, F.A., Ul-Haq, R., Al-Mdallal, Q.M., Zhang, Q., Heat generation/absorption and nonlinear radiation effects on stagnation point flow of nanofluid along a moving surface, *Results Phys.*, 8, 2018, 404–414.
[37] Malik, M.Y., Khan, I., Hussain, A., Salahuddin, T., Mixed convection flow of MHD Eyring-Powell nanofluid over a stretching sheet: A numerical study, *AIP Advances*, 5, 2015, 1-14.
[38] Akbar, N.S., Ebaid, A., Khan, Z.H., Numerical analysis of magnetic field effects on Eyring-Powell fluid flow towards a stretching sheet, *Journal of Magnetism and Magnetic Materials*, 382, 2015, 355-358.
[39] Ara, A., Khan, N.A., Khan, H., Sultan, F., Radiation effect on boundary layer flow of an Eyring-Powell fluid over an exponentially shrinking sheet, *Ain Shams Engineering Journal*, 5, 2014, 1337-1342.
[40] Javid, T., Ali, N., Abbas, Z., Sajid, M., Flow of an Eyring-Powell non-Newtonian fluid over a stretching sheet, *Chemical Engineering Communications*, 3, 2012, 327-336.
[41] Akbar, N.S., Nadeem, S., Haq, R.U., Khan, Z.H., Numerical solutions of magnetohydrodynamic boundary layer flow of tangent hyperbolic fluid towards a stretching sheet, *Indian Journal of Physics*, 87, 2013, 1121-1124.
[42] Nadeem, S., Haq, R.U., Lee, C., MHD boundary layer flow over an unsteady shrinking sheet: an analytical and numerical approach, *Journal of the Brazilian Society of Mechanical Sciences and Engineering*, 37, 2015, 1339-1346.
[43] Malik, M.Y., Naseer, M., Nadeem, S., Rehman, A., The boundary layer flow of Casson nanofluid over a vertical exponentially stretching cylinder, *Applied Nanoscience*, 4, 2014, 869-873.
[44] Khan, W.A., Pop, I., Boundary-layer flow of a nanofluid past a stretching sheet, *International Journal of Heat and Mass Transfer*, 53, 2010, 2477-2483.
[45] Nadeem, S., Mehmood, R., Akbar, N.S., Non-orthogonal stagnation point flow of a nano non-Newtonian fluid towards a stretching surface with heat transfer, *International Journal of Heat and Mass Transfer*, 57, 2013, 679-689.
[46] Abolbashari, M.H., Freidoonimehr, N., Nazari, F., Rashidi, M.M., Analytical modeling of entropy generation for Casson nano-fluid flow induced by a stretching surface, *Advanced Powder Technology*, 26, 2015, 542-552.
[47] Akbar, N.S., Nadeem, S., Lee, C., Khan, Z.H., Haq, R.U., Numerical study of Williamson nanofluid flow in an asymmetric channel, *Results in Physics*, 3, 2013, 161-166.
[48] Dalir, N., Dehsara, M., Nourazar, S.S., Entropy analysis for magnetohydrodynamic flow and heat transfer of a Jeffrey nanofluid over a stretching sheet, *Energy*, 79, 2015, 351-362.
[49] Freidoonimehr, N., Rashidi, M.M., Mahmud, S., Unsteady MHD free convective flow past a permeable stretching vertical surface in a nano-fluid, *International Journal of Thermal Sciences*, 87, 2015, 136-145.
[50] Abolbashari, M.H., Freidoonimehr, N., Nazari, F., Rashidi, M.M., Entropy analysis for an unsteady MHD flow past a stretching permeable surface in nano-fluid, *Powder Technology*, 267, 2014, 256-267.
[51] Hakeem, A.K.A., Ganesh, N.V., Ganga, B., Magnetic field effect on second-order slip flow of nanofluid over a stretching/shrinking sheet with thermal radiation effect, *Journal of Magnetism and Magnetic Materials*, 381, 2015, 243-257.
[52] Malvandi, A., Hedayati, F., Ganji, D.D., Slip effects on unsteady stagnation point flow of a nanofluid over a stretching sheet, *Powder Technology*, 253, 2014, 377-384.
[53] Sheikholeslami, M., Jafaryar, M., Alsabery, Z.A.I, Shafee, H.B.A., Modification for helical turbulator to augment heat transfer behavior of nanomaterial via numerical approach, *Applied Thermal Engineering*, 182, 2021, 115935.
[54] Sheikholeslami, M., Farshad, S.A., Shafee, A., Babazadeh, Performance of solar collector with turbulator involving nanomaterial turbulent regime, *Renewable Energy*, 163, 2021, 1222-1237.
[55] Narender, G., Govardhan, K., Sarma, G.S., MHD Casson Nanofluid Past a Stretching Sheet with the Effects of Viscous Dissipation, Chemical Reaction and Heat Source/Sink, *J. Appl. Comput. Mech.*, 2021, DOI: 10.22055/JACM.2019.14804.
[56] Mabood, F., Bognár, G., Shafiq, A., Impact of heat generation/absorption of magnetohydrodynamics Oldroyd-B fluid impinging on an inclined stretching sheet with radiation, *Scientific Reports*, 10, 2020, 1–12
[57] Shoaib, M., Raja, M.A.Z., Sabir, M.T., Islam, S., Shah, Z., Kumam, P., Alrabaiah, H., Numerical investigation for rotating flow of MHD hybrid nanofluid with thermal radiation over a stretching sheet, *Scientific Reports*, 10, 2020, 18533.
[58] Ullah, I., Khan, I., Shafie, S., Soret and Dufour effects on unsteady mixed convection slip flow of Casson fluid over a nonlinearly stretching sheet with convective boundary condition, *Scientific Reports*, 7, 2017, 1–19.
[59] Hamid, R.A., Nazar, R., Pop, I., Non-alignment stagnation-point flow of a nanofluid past a permeable stretching/shrinking sheet: Buongiorno's model, *Scientific Reports*, 5, 2015, 1–11.
[60] Zaimi, K., Ishak, A., Pop, I., Boundary layer flow and heat transfer over a nonlinearly permeable stretching/shrinking sheet in a nanofluid, *Scientific Reports*, 4, 2014, 1–8.
[61] Mukhopadhyay, S., De, P.R., Bhattacharyya, K., Layek, G.C., Casson fluid flow over an unsteady stretching surface, *Ain Shams Eng. J.*, 4, 2013, 933–938.
[62] Mabood, F., Khan, W.A., Ismail, I.A.M., MHD boundary layer flow and heat transfer of nanofluids over a nonlinearly stretching sheet: a numerical study, *Journal of Magnetism and Magnetic Materials*, 374, 2015, 659-576.
[63] Khan, M., Malik, M.Y., Salahuddin, T., Heat generation and solar radiation effects on Carreau nanofluid over a stretching sheet with variable thickness: Using coefficients improved by Cash and Carp, *Results in Physics*, 7, 2017, 2512-2519.

ORCID iD

Ram Prakash Sharma https://orcid.org/0000-0002-3359-1316
Sachin Shaw https://orcid.org/0000-0002-5456-8596

How to cite this article: Sharma R.P., Shaw S. MHD Non-Newtonian Fluid Flow past a Stretching Sheet under the Influence of Non-linear Radiation and Viscous Dissipation, *J. Appl. Comput. Mech.*, 8(3), 2022, 949–961.
https://doi.org/10.22055/JACM.2021.34993.2533